GL04034

DERIVATION OF AN ISOTOPIC RATE MODEL

by

David R. Cole

1981

INTRODUCTION

The isotopic ratios of $^{18}O/^{16}O$ and D/H have been increasingly used to resolve reaction paths of mineral-fluid reactions occurring both in the laboratory and in nature. Isotopic exchange between minerals and fluids has been attributed to one of two major processes, dissolution-reprecipitation or diffusion. Of these two mechanisms, diffusion of oxygen or oxygen-bearing species such as H_2O or OH^- in silicates has received the most attention in recent years. Diffusion coefficients for oxygen (or oxygen-bearing species) have been determined for a variety of mineral-fluid systems, including feldspars (Merigoux, 1968; Anderson and Kasper, 1975; Yund and Anderson, 1974, 1978; Giletti et al., 1978), phlogopite (Giletti and Anderson, 1975) and magnetite (Castle and Surman, 1969). These studies contend that when minerals and fluids are in chemical equilibrium, oxygen isotopic exchange can only occur through a diffusional mechanism. The attainment of chemical equilibrium in many of these experiments is uncertain due to the lack of supporting evidence (e.g. chemical analyses of solids and fluids, x-ray, SEM).

In contrast, isotopic exchange in mineral-fluid systems that are far from chemical equilibrium is controlled by solution-redeposition. Experimental reactions between high-temperature chloride solutions and feldspars studied by O'Neil and Taylor (1967) and Merigoux (1968) indicate that Na-K ion exchange is always accompanied by oxygen isotopic exchange. O'Neil and Taylor (1967) identified the mechanism of this exchange as a fine-scale recrystallization involving

a reaction front moving through the crystal with local dissolution and redeposition in a fluid film at the interface between the exchanged and unexchanged feldspar. The electron microprobe data from their experiments indicate that alkali-chloride solutions had access to the interior of the crystals along cleavage cracks and newly formed surfaces of discontinuity. This implies that armoring of the original grain by secondary depositional products did not severely restrict communication between the aqueous fluid and the unexchanged feldspar.

A similar phenomenon of solution-recrystallization was observed for isotopic experiments that involved the reaction of carbonates with aqueous chloride solutions or pure water (O'Neil et al., 1969; Northrop and Clayton, 1966; Anderson and Chai, 1974), paragonite with KCl solutions (O'Neil and Taylor, 1969), quartz with NaF solutions (Clayton et al., 1972), and barite with NaCl or NaCl plus H_2SO_4 solutions (Kusakabe and Robinson, 1977). These experiments and those involving recrystallization of feldspars were not designed specifically to measure rates of isotopic exchange. Mineralogic and x-ray diffraction data obtained from these experiments suggest that any kinetic theory developed to quantify rates of isotopic exchange in systems undergoing mineralogic change must account for the surface-exchange phenomenon.

This study was undertaken to develop a basis for oxygen or hydrogen isotopic reaction kinetics that is consistent with a model of surface dissolution-reprecipitation. The simplified differential rate equation that is derived indicates the rate of isotopic exchange to be

proportional to the degree of isotopic equilibrium and the product of the number of moles of oxygen (hydrogen) in water and the mineral, and inversely proportional to the surface area of the mineral, the total number of moles of oxygen (hydrogen) in the system (water plus mineral) and time. Estimates of oxygen isotopic rate constants are made for a variety of experimental mineral-fluid systems (e.g., feldspar-fluid, calcite-fluid), where dissolution-reprecipitation reactions were observed. The estimation of hydrogen isotopic rate constants will be addressed in the next paper of this series. The principal difficulty in using data from the literature is that in no case was the surface area measured for either reactants or products. Therefore, surface areas used in the calculations are only estimates based on assumed grain geometries.

In addition, a detailed examination is made into factors that control diffusional isotopic exchange. In previous studies (e.g., Giletti et al., 1978), the rate of isotopic equilibration of oxygen (or oxygen-bearing species) diffusing from a fluid into a particular phase was modeled for systems where only temperature and grain size were considered. It can be shown from a rigorous treatment of diffusion of a solute into a solid, that in addition to grain geometry the magnitude of the volume of solution to volume of solid ratio also contributes to the rate of equilibration (see Crank, 1975). According to Crank (1975) this volume ratio must be corrected for the equilibrium partition of the exchanging species between fluid and solid in terms of concentration. Diffusion equations are given for various

grain geometries that demonstrate these relations.

Finally, the equations derived for both diffusion and surface-isotopic exchange are used to compute the change in the degree of isotopic equilibration (F) with time for systems of specified temperatures, water/mineral mass ratios and grain sizes. The water/mineral volume ratios used originally in the diffusion equations are easily converted to mass ratios if the density of both the solution and solid are known. Similarly, if density and grain geometry are known, the isotopic rate equation for surface exchange can be recast to incorporate water/mineral mass ratios rather than concentrations. These manipulations facilitate a more direct comparison of the two mechanisms for similarly defined systems. This comparison is used to illustrate how isotopic exchange can occur in various natural environments (e.g., geothermal, ore deposit, metamorphic).

NOMENCLATURE

A	interfacial area (m^2)
A'	pre-exponential term in Arrhenius equation
$(C_n)_j$	concentration of n isotope (^{18}O, ^{16}O, D, H) of the jth phase (water, solid)
C_o	initial concentration of solute (oxygen or oxygen-bearing species) prior to diffusion into solid
D	diffusion coefficient ($cm^2 sec^{-1}$)
E_{act}	activation energy (Kcal mol^{-1})
F	fractional approach to isotopic equilibrium
K	equilibrium constant for dissociation reaction
K'	equilibrium isotope partition ratio between solid and water corrected for concentration
M_s	mass of solid in experimental run (gm)
N	number of grains comprising reactant
R	gas constant (1.987 cal mol^{-1} K^{-1})
S_1	number of atoms of $^{16}O(H)$ in solid
S_2	number of atoms of $^{18}O(D)$ in solid
S	number of moles of oxygen (hydrogen) in solid
T	temperature (K)
V_s	volume of solid ($1.333\pi a^3$ for sphere, bwh for plate; cc)
V_w	volume of water (cc)
W	number of moles of oxygen (hydrogen) in water
W_1	number of atoms of $^{16}O(H)$ in water
W_2	number of atoms of $^{18}O(D)$ in water
(W/S)	mole ratio of oxygen (hydrogen) in water to that in solid

$(W/S)_m$	mass ratio of water to solid
X_s	total number of moles of oxygen in solid
a	radius of spherical grain or sheet (cm)
b	base; the edge of an octagonal plate or the long dimension of a rhomb (cm)
e	superscript signifiyng equilibrium
h	height; radius of an octagonal plate or height of a rhomb (cm)
i	superscript signifying initial
k_+	dissolution rate constant (moles $m^{-2}sec^{-1}$)
k_-	precipitation rate constant (moles $m^{-2}sec^{-1}$)
g_n	non-zero roots used in Laplace transform
r_1	isotopic rate constant of the forward reaction (moles $m^{-2}sec^{-1}$)
r_2	isotopic rate constant of the reverse reaction (moles $m^{-2}sec^{-1}$)
t	time (sec)
w	plate or rhomb thickness (cm)
1	subscript signifying $^{16}O(H)$
2	subscript signifying $^{18}O(D)$
α_{sw}	isotopic fractionation factor between solid and water
β	volume of water to volume of solid ratio
ρ	density (gm cc^{-1})
$\delta^{18}O$	$= [(^{18}O/^{16}O)_j - (^{18}O/^{16}O)_{std}/(^{18}O/^{16}O)_{std}]10^3$ in °/oo

Abstract

A rate equation for isotopic (oxygen, hydrogen) exchange between minerals and water has been derived based on a model of addition or removal of atoms from the surface of the solid. Rate constants (moles m^{-2} sec^{-1}) for oxygen isotopic exchange accompanying surface reactions (dissolution, precipitation) in mineral-fluid systems are obtained from the rate equation

$$r = -\ln(1-F)(WS)/(W+S)(t)(A)$$

where W and S are the moles of oxygen in the solution and solid, respectively, A is the surface area of the mineral (m^2), t is time (sec) and F is the degree of equilibrium. Typical rate constants for oxygen isotopic exchange between common silicates (feldspars, quartz, micas) or carbonates (calcite, dolomite) and solutions plot between 10^{-4} and 10^{-8} moles m^{-2} sec^{-1}, with activation energies ranging from 8 to 22 Kcal $mole^{-1}$.

These rate constants for surface exchange are used to compute the times required to attain 90% exchange for systems with varying grain radii, mineral/fluid mass ratios, and temperatures. The results of these calculations are compared with times computed from diffusion equations. This comparison indicates that the time required to reach isotopic equilibrium increases with an increase in the fluid/mineral mass ratio and/or grain size, and a decrease in temperature, regardless of the mechanism. Diffusion-controlled oxygen isotopic exchange, however, is several orders of magnitude slower than isotopic exchange accompanying surface reactions.

DERIVATION OF AN ISOTOPIC RATE MODEL

In order to quantify the rates of isotopic exchange during dissolution-reprecipitation, a model is developed to describe the kinetics of mineral-fluid interaction which are applicable to isotopic exchange at any fluid-solid interface. Because an isotopic exchange reaction is a chemical reaction in which atoms of a given element interchange between two or more chemical forms of the element, any calculation of the rate of isotopic exchange has to make use of a general theory of reaction rates. The absolute reaction rate theory as presented, for instance, by Glasstone et al. (1941) has proved useful for this purpose. Its limitation in practical cases, such as mineral hydrolysis or reprecipitation, lies in our incomplete knowledge of the actual transition states involved and the difficulty at present of making quantum-mechanical calculations accurate enough for any but the simplest systems. For a detailed discussion of the application of transition state theory to the kinetics of mineral hydrolysis refer to Lasaga (1981).

The isotopic relationships for fluid-mineral interaction important in the development of a kinetic model are given in the following schematic bar graph

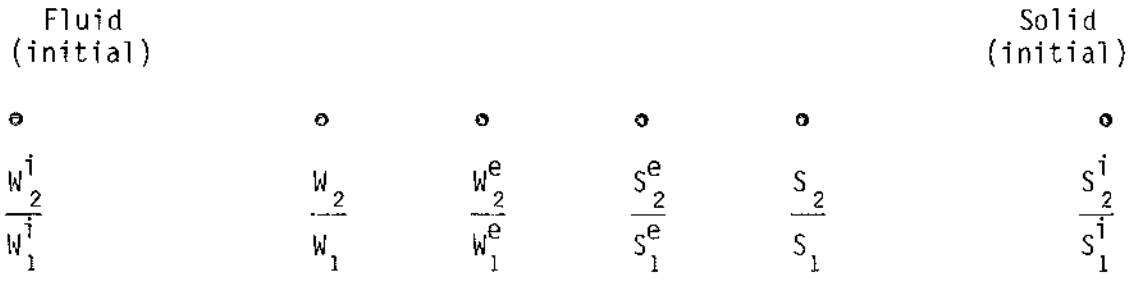

where the isotopic ratios (W_2^i/W_1^i) and (S_2^i/S_1^i) represent the initial isotopic composition of the fluid and solid, respectively; the ratios (W_2/W_1) and (S_2/S_1) refer to compositions of fluid and solid observed at some time (t) during the reaction and (W_2^e/W_1^e) and (S_2^e/S_1^e) are the equilibrium isotopic ratios of fluid and solid, respectively.

Because the number of atoms of $^{16}O(H)$ is much greater than the number of $^{18}O(D)$ atoms in water and solid (e.g., silicates, carbonates, sulfates), we can assume that

$$W_1^i \simeq W_1 \simeq W_1^e \ (\simeq W = W_1 + W_2) \tag{1}$$

and

$$S_1^i \simeq S_1 \simeq S_1^e \ (\simeq S = S_1 + S_2) \tag{2}$$

The isotopic composition of the system can be shown as

$$\left(\frac{^{18}O}{^{16}O}\right)_{sys} = \frac{S_2^i + W_2^i}{S_1^i + W_1^i} = \frac{S_2 + W_2}{S_1 + W_1} = \frac{S_2^e + W_2^e}{S_1^e + W_1^e} \tag{3}$$

with

$$S_2 + W_2 = S_2^e + W_2^e \tag{4}$$

The equation for the oxygen (hydrogen) isotopic exchange reaction between solid and fluid can be written as

$$S_2 + W_1 \underset{r_2}{\overset{r_1}{\rightleftarrows}} S_1 + W_2 \tag{5}$$

where r_1 and r_2 are the rate constants of the forward and reverse reactions, respectively. If the rate-limiting step is the addition and removal of oxygen (hydrogen) atoms from the surface of the solid, then the rate of change in the concentration of W_2 in reaction (5) at time t can be expressed as

$$\frac{dW_2}{dt} = r_1 A(C_2)_s (C_1)_w - r_2 A(C_1)_s (C_2)_w \tag{6}$$

The parameter, A, is the total surface area of the solid phase in m^2 for the system. From the following identities,

$$(C_2)_s = \frac{S_2}{S_1+S_2} = \frac{S_2}{S} \tag{7}$$

$$(C_1)_s = \frac{S_1}{S} \tag{8}$$

$$(C_2)_w = \frac{W_2}{W} \tag{9}$$

$$(C_1)_w = \frac{W_1}{W} \tag{10}$$

substitution into equation (6) gives

$$\frac{dW_2}{dt} = A \left[r_1 \frac{S_2}{S} \frac{W_1}{W} - r_2 \frac{S_1}{S} \frac{W_2}{W} \right] \tag{11}$$

which simplifies to

$$\frac{dW_2}{dt} = \frac{A}{SW} (r_1 S_2 W_1 - r_2 S_1 W_2) \tag{12}$$

By recalling the definition of the equilibrium fractionation factor between solid and fluid as

or

$$\alpha_{sw} = \frac{r_2}{r_1} \tag{13}$$

$$\alpha_{sw} r_1 = r_2 \tag{14}$$

and substituting equation (14) into equation (12), the following is given

$$\frac{dW_2}{dt} = \frac{Ar_1}{SW} (S_2 W_1 - \alpha_{sw} S_1 W_2) \tag{15}$$

From equation (4)

$$S_2 = S_2^e + W_2^e - W_2 \tag{16}$$

which can be used in equation (15) to yield

$$\frac{dW_2}{dt} = \frac{Ar_1}{SW} W_1 (S_2^e + W_2^e - W_2) - \alpha_{sw} W_2 S_1 \tag{17}$$

or

$$\frac{dW_2}{dt} = \frac{Ar_1}{SW} W_1 (W_2^e - W_2) + W_1 S_2^e - \alpha_{sw} W_2 S_1 \tag{18}$$

Rewriting the equilibrium fractionation factor, α_{sw}, in the form

$$\alpha_{sw} = \frac{S_2^e / S_1^e}{W_2^e / W_1^e} \approx \frac{S_2^e / S_1}{W_2^e / W_1} \tag{19}$$

or

$$W_1 S_2^e = \alpha_{sw} S_1 W_2^e \tag{20}$$

equation (18) can be recast into

$$\frac{dW_2}{dt} = \frac{Ar_1}{SW} W_1 (W_2^e - sW_2) + \alpha_{sw} S_1 W_2^e - \alpha_{sw} W_2 S_1 \tag{21}$$

which reduces to

$$\frac{dW_2}{dt} = \frac{Ar_1}{SW}(W_2^e - W_2)(W_1 + \alpha_{sw}S_1) \tag{22}$$

Rearranging equation (22), we get

$$\frac{dW_2}{(W_2^e - W_2)} = \frac{Ar_1}{SW}(W_1 + \alpha_{sw}S_1)dt \tag{23}$$

The integrated form of equation (23) is

$$\ell n(W_2^e - W_2) = \frac{Ar_1}{SW}(W_1 + \alpha_{sw}S_1)t + \text{constant} \tag{24}$$

The integration constant can be evaluated at t=0 when $W_2 = W_2^i$ (the initial value prior to reaction)

$$\text{constant} = -\ell n(W_2^e - W_2^i) \tag{25}$$

Substituting (25) into equation (24) and rearranging yields

$$\frac{r_1 tA}{SW} = -\frac{1}{(W_1 + \alpha_{sw}S_1)} \ell n \frac{(W_2^e - W_2^i) - (W_2 - W_2^i)}{(W_2^e - W_2^i)} \tag{26}$$

which simplifies to

$$\frac{r_1 tA}{SW} = -\frac{1}{(W_1 + \alpha_{sw}S_1)} \ell n \left(1 - \frac{(W_2 - W_2^i)}{(W_2^e - W_2^i)}\right) \tag{27}$$

By definition

$$F = \frac{(W_2 - W_2^i)}{(W_2^e - W_2^i)} \tag{28}$$

and is the fraction of isotopic exchange, which can be substituted into equation (27) to give

$$\frac{r_1 tA}{SW} = -\frac{1}{(W_1 + \alpha_{sw} S_1)} \ell n(1-F) \qquad (29)$$

In this equation, (1-F) is a measure of the departure from equilibrium. Note that when F=0, there has been no exchange ($W_2 = W_2^i$) and at equilibrium ($W_2 = W_2^e$), or 100% exchange, F=1.

As a first approximation, we can assume that $\&_{sw}$ is essentially equal to one and $W_1 + S_1 \simeq W + S$. Then equation (29) simplifies to

$$\frac{r_1 tA}{SW} = -\frac{1}{(W+S)} \ell n(1-F) \qquad (30)$$

Solving for the rate constant we get

$$r_1 = \frac{-\ell n(1-F)(SW)}{(W+S)tA} \qquad (31)$$

where r_1 is expressed as mole $m^{-2}sec^{-1}$. In order to determine rate constants from experiments, the surface area of the solid, moles of oxygen (or hydrogen) in solution and solid and the fraction of isotopic exchange at some time t must be known.

Once the isotopic rate constants at various temperatures are derived from equation (31) for a given dissolution-reprecipitation reaction, the activation energy (E_{act}) for the reaction can be calculated from the Arrhenius equation

$$\log r_1 = \frac{-E_{act}}{2.3\ RT} + \log A' \qquad (32)$$

where A' is the pre-exponential factor. It apparently has little or

no temperature dependence and thus can be considered a constant.

CALCULATION OF RATE CONSTANTS FOR SELECTED EXPERIMENTAL SYSTEMS

Problems and assumptions

Values of r_1 are estimated for selected oxygen isotopic exchange experiments described in the literature using equation (31). In order to use this equation effectively, data on isotopic concentrations versus time are required from systems where P, T, A, W, S and reaction products are known. Most isotopic exchange experiments described for mineral-fluid systems exhibiting redeposition measured equilibrium isotopic fractionation factors ($\&_{sw}$), not rates of exchange. In no case was the isotopic concentration monitored through time nor the surface area of reactants measured. In addition, the masses of solid and fluid used in each experimental run are not given, but instead described only in general terms (i.e., a typical run charge consisted of 10 mg of solid, 100 mg of solution).

Of the remaining parameters required for the use of equation (31), data on the fraction of exchange (F), time (t) and temperature are usually documented in detail. The presence of a secondary run product or recrystallized reactant has been verified by either x-ray or microscopic examination for most oxygen isotopic experiments not designed to measure diffusion coefficients.

Various assumptions are made that permit the application of the isotopic rate equation (31) to a wide spectrum of literature results.

(1) We can assume for the sake of comparison that all partial

isotopic exchange observed in experiments that did not specifically address diffusion resulted from redeposition or recrystallization-type reactions. This assumption is most applicable to experiments where the technique of partial oxygen isotopic exchange was employed to estimate equilibrium fractionation factors (e.g., O'Neil and Taylor; 1967, 1969). Oxygen isotopic exchange by means of diffusion in silicates and oxides is evaluated in a later section and compared to rates computed from equation (31).

(2) In order to use equation (31), the moles of oxygen (or hydrogen) in the solution (W) and solid (S) are required. Ideally, the mass of solution and solid are known for each experimental run from which the number of moles of oxygen or hydrogen can be computed. With the exception of the study by Kulla (1979), run conditions for individual experiments are not given. Instead, an average mass of solution and solid are described, from which the moles of oxygen (or hydrogen) have been calculated.

(3) As indicated previously, surface areas of reactants have not been measured in any of the isotopic exchange experiments described in the literature. Typically, argon or nitrogen BET measurements are used as standard techniques for determining the relative surface areas of solids. These techniques generally give higher values for the surface areas than would be calculated from geometrical considerations of individual grains because the gas adsorption measurements are sensitive to surface roughness and porosity (Rimstidt and Barnes, 1980). Surface areas used in the calculation of rates of isotopic exchange

are estimated from the following formulas assuming certain grain geometries.

For a sphere

$$A(m^2) = (4\pi a^2)\left(\frac{Ms}{\rho \cdot 1.33\pi a^3}\right) \quad 10^4 \tag{33}$$

where the first term within the brackets gives the area of one sphere of radius (a) in cm and the second term computes the number of grains. The values of (a) are either taken directly from grain sizes given in each paper or estimated from the average sieve size used, where (a) equals one half of the sieve opening dimension. A spherical model is adopted for all feldspar, quartz, glass, and barite, experiments unless other geometries are documented.

For a rhombohedron

$$A(m^2) = (bh)\left(\frac{Ms}{\rho \cdot bhw}\right) \quad 10^4 \tag{34}$$

It is assumed for rhombohedron grains that (b), the base, equals the average sieving opening dimension, (h) the height equals 0.65b and the width (w) equals 0.5(b). Although these proportions are somewhat arbitrary, they are based on the shape of a typical Iceland spar calcite rhomb.

For an octagonal plate

$$A(m^2) = (4bh)\left(\frac{Ms}{\rho \cdot 4bhw}\right) \quad 10^4 \tag{35}$$

where the height (h) equals one half of the sieve opening dimension, the base (b) equals approximately 0.8h and the width (w) equals 0.1b. These proportions are based, in part, on the description of

muscovite and paragonite run material (O'Neil and Taylor, 1969) and clay reactants described by O'Neil and Kharaka (1976). This model was used for clays and other phyllosilicates if reactants or products were described in detail. Otherwise, a spherical grain geometry was employed. The difference in surface areas computed for a given experiment using the various models averaged less than 5%.

(4) The fraction of isotopic exchange (F) given for each set of experimental runs was used directly in the rate equation (31). No attempt is made to verify the level of precision or accuracy attained in these experiments.

(5) Finally, in order to test the validity of equation (31), it is necessary to obtain data on isotopic concentration versus time as the mineral-fluid interaction proceeds. With the exception of a study on isotopic redistribution during calcite recrystallization by Anderson and Chai (1974), experimental data of this type are lacking in the literature. The determination of isotopic rate constants for a recrystallization process is illustrated with data from experiments conducted by Anderson and Chai (1974) at 305, 400 and 500°C (Fig. 1).

By recasting equation (31) to solve for t

$$t = \frac{-\ln(1-F)\ WS}{r_1(W+S)\ A} \qquad (36)$$

we see that it is a linear equation of the form $y = mx$, where $m = -WS/r_1(W+S)A$ and $x = \ln(1-F)$. Therefore, if $\ln(1-F)$ is plotted versus elapsed time and $WS/(W+S)A$ is constant, the slope of the line will be $-1/r_1$. Unfortunately, Anderson and Chai (1974) did not sample the

same experiment through time, but instead conducted individual experiments at the same temperature for different durations. In addition, the grain sizes they employed varied from one run to another. Consequently, individual rate constants are calculated from equation (31) for each capsule run for all of their experiments. This same approach is adopted for all other literature results. The only reliable check we have on the validity of this approach is if we compute similar rate constants for experiments with different run conditions (i.e., different W, S, A, t, F), but where run products are chemically and mineralogically similar.

For a summary of run conditions and parameters used in equation (31), see Table 1. In cases where it was not clear whether recrystallization or deposition actually took place, the proposed product phase is bracketed with parentheses.

$^{18}O/^{16}O$ rates of exchange between mineral and fluid

The oxygen isotopic rate constants calculated from equation (31) for most mineral-fluid experiments described in Table 1 have been plotted on Arrhenius plots (Fig. 2 and 3). Each rate value given in these plots represents an individual run or group of runs for which a fraction of isotopic exchange was determined. From equation (32), it can be seen that the result should be a linear function if the reaction mechanism is unchanged over the temperature range of interest. Straight lines have been regressed through the data for each individual reaction (e.g., Albite + 3M kCl = Kspar + 3M NaCl) in the form

$$\log r_1 = a(10^3/T) - b \qquad (37)$$

where a is the slope of the line and b is the intercept. From the slopes of these lines, $a = (-Eact/R(2.3 \times 10^3))$, the activation energies for oxygen isotopic exchange controlled by recrystallization or deposition reactions are calculated. Table 2 summarizes the various reactions, equations for the regression lines, the regression coefficients and the activation energies for oxygen isotopic exchange.

Lines fit to feldspar-salt solution data (Fig. 2a) derived from O'Neil and Taylor (1967) indicate that below about 500°C, the rates of oxygen isotopic exchange accompanying new mineral growth resulting from Na-K ion exchange (i.e., Kspar after albite or albite after sanidine) are indistinguishable. Conversion of celsian ($BaAl_2Si_2O_8$) to anorthite resulted in rate constants for isotopic exchange that are approximately one order of magnitude lower than the other feldspar-salt solution reactions. Sanidine and albite reacted with either pure water or a salt solution in equilibrium with the crystals (Fig. 2b) resulted in rate constants generally one order of magnitude lower than those calculated for feldspar-salt solution experiments. Activation energies range from 17.5 to 25.6 and 17.2 and 21.2 kcal mol^{-1} for feldspar-salt solution and feldspar-pure water isotopic exchange, respectively. These activation energies are comparable to those observed for dissolution of feldspars (Lasaga, 1981).

O'Neil and Taylor (1967) defend the concept that some dissolution-redeposition occurred in their feldspar-pure water runs. No mineralogic evidence was obtained, however, to substantiate this claim. Whether the total fraction of oxygen isotopic exchange can be

contributed entirely to such a process is still uncertain. It is possible that volume diffusion of an oxygen-bearing species into the feldspars also contributed to the observed isotopic exchange.

Interestingly, rate constants computed from albite-pure water data given by Matsuhisa et al. (1979) plot virtually on top of the rate constants estimated from the O'Neil and Taylor (1967) albite-pure water data, even though the former set of experiments were conducted at 15kb and the latter only at 1kb. Yund and Anderson (1978) demonstrated convincingly that oxygen diffusion coefficients have a positive dependence on fluid pressure. A similar relationship between fluid pressure and oxygen diffusion was documented by Castle and Surman (1969) in their study of magnetite. If diffusion was the principal mechanism involved in albite-pure water isotopic exchange, the relationships observed in Fig. 2b should not occur. Consequently, dissolution-reprecipitation is probably the dominant mechanism controlling oxygen isotopic exchange in the feldspar-pure water experiments, as well as the feldspar-salt solution runs.

Quartz-pure water and quartz-NaF rate constants are shown in Fig. 2c. In the quartz-NaF experiments (dashed lines), Clayton et al. (1972) observed extensive recrystallization of quartz. The separation of rate constants derived from the Clayton et al. (1972) experiments into two populations (Fig. 2c) has apparently resulted from the use of different types of quartz starting materials. Other than their oxygen isotopic composition, the exact nature of the differences between the various quartz materials, such as surface roughness, dislocations or

fractures, is not known.

Rate constants derived from the quartz-pure water data of Matsuhisa et al. (1979) plot very close to the upper quartz-NaF rate line (Fig. 2c). The quartz-pure water rate constant calculated from data given by Clayton et al. (1972) is approximately one order of magnitude lower than similar rate constants computed from the Matsuhisa et al. (1979) data. Experiments by Clayton et al. (1972) were carried out at 1kb, whereas Matsuhisa et al. (1979) conducted their experiments at 2 and 15kb. The difference in the rate constants calculated for quartz-pure water isotopic exchange might be explained by the 14kb pressure difference between the two data sets if diffusion was the dominate mechanism, and not recrystallization. However, the fact that the 2kb, 700°C run of Matsuhisa et al. (1979) yields a rate constant similar to the 15kb, 700°C experiment and, at the same time plots on the upper quartz-NaF regression line, suggests that recrystallization, not diffusion, is probably the dominate mechanism. The lower rate constant for quartz-pure water derived from the data of Clayton et al. (1972) can probably be attributed to starting material variations discussed above.

The activation energies calculated for quartz-pure water and quartz-NaF oxygen isotopic exchange are approximately 10.8 and 5.4 kcal mol^{-1}, respectively. An activation energy of 11.9 kcal mol^{-1} is given by Rimstidt and Barnes (1980) for quartz deposition from pure water.

Rate constants for paragonite-salt solution and kaolinite-NaCl

oxygen isotopic exchange are plotted in Fig. 2d. Extensive redeposition was observed in both of these sets of experiments (i.e., muscovite from paragonite, diaspore plus pyrophyllite from kaolinite). In one case, paragonite was recrystallized from muscovite reacted with 3M NaCl at 500°C. The rate constant for this experiment is nearly identical to that obtained for the paragonite-3M KCl run at 500°C. These data suggest that oxygen isotopic exchange accompanying Na-K ion exchange in micas can be modeled from the line fit to these data, which yields an activation energy of 14.8 kcal mol^{-1}.

Experiments involving kaolinite alteration to diaspore plus pyrophyllite yield isotopic rate constants similar in magnitude to the rate constants computed or extrapolated for mica-salt solution isotopic exchange. An activation energy of 9.8 kcal mol^{-1} is estimated for the kaolinite reaction (Table 3).

Rate constants for oxygen isotopic exchange between carbonates and various types of solutions are given in Figs. 3a, 3b, and 3c. Calcite-pure water isotopic rate constants computed from data given by Anderson and Chai (1974) are in excellent agreement with rates predicted for oxygen isotopic exchange in the systems, calcite-NH_4Cl and calcite-pure water from data given by O'Neil *et al.* (1969). In both series of experiments, extensive recrystallization of calcite was observed. Activation energies range from 6.3 to 10.4 kcal mol^{-1} for experiments conducted by O'Neil *et al.* (1969) and Anderson and Chai (1974), respectively. Sjoberg (1976) gives an activation energy of 8.4 kcal mol^{-1} for calcite dissolution.

Dolomite reacted with NH_4Cl resulted in the recrystallization of dolomite and the formation of minor amounts of Mg-calcite (Northrop and Clayton, 1966). The rates of isotopic exchange computed from these experiments (Fig. 3b) are nearly identical to the calcite-pure water rate data shown in Fig. 3a. An activation energy of 10.9 kcal mol^{-1} is calculated from these dolomite-NH_4Cl data.

The rate of oxygen isotopic exchange between dolomite and pure water is approximately one order of magnitude lower than exchange between dolomite and NH_4Cl solutions. As with the feldspar rate data, it is possible that a line representing the dolomite-pure water rates of oxygen isotopic exchange could lie one order of magnitude below the line defining dolomite-salt solution isotopic exchange, but with a similar slope. More experimental work is needed, however, to verify this empirical observation.

Rate constants for other carbonates, strontianite ($SrCO_3$) and witherite ($BaCO_3$) are summarized in Fig. 3c. Although the data are limited, the magnitude of the rate constants for oxygen isotopic exchange appear to be about one order of magnitude higher than calcite-pure water or dolomite-NH_4Cl. As with these latter systems, strontianite and witherite underwent extensive recrystallization during hydrothermal interaction with NH_4Cl solutions (O'Niel et al., 1969). Activation energies for these isotopic reactions range from 6.4 kcal mol^{-1} for strontianite-NH_4Cl to 10.2 kcal mol^{-1} for witherite-NH_4Cl. Interestingly, one rate constant calculated for aragonite-NH_4Cl isotopic exchange plots very near the line regressed

through the strontianite-NH_4Cl rate data. This may be explained, in part, by the fact that both strontianite and witherite have structural configurations similar to aragonite (Deer et al., 1966) and could exhibit similar crystallization characteristics.

Rate constants for oxygen isotopic exchange in the systems barite-NaCl and barite-NaCl plus H_2SO_4 are given in Fig. 3d. Kusakabe and Robinson (1977) noted widespread recrystallization of barite in their hydrothermal experiments. It is readily apparent that exchange rates are higher in the barite-NaCl plus H_2SO_4 system. Kusakabe and Robinson (1977) attribute these higher rates of exchange to the inreased solubility of barite in NaCl plus H_2SO_4 solutions. At temeratures below about 200°C, the difference in rate constants between the two systems is at least one order of magnitude. This difference becomes smaller with increasing temperature because the rate lines converge.

The rate data given in Fig. 3d for each experimental system (i.e., barite-NaCl or barite-NaCl plus H_2SO_4) can be partitioned into two populations and fit with separate regression lines. This suggests that oxygen isotopic exchange is controlled by a more complex phenomenon than simple recrystallization. It is possible that rapid recrystallization at higher temperatures (greater than 200°C) with subsequent armoring of reactant materials impedes the process of dissolution-redeposition. Consequently, transfer of material would occur by diffusion through the surface coating of newly crystallized barite.

For ease of comparison, regression lines have been fit to all the data computed from each experimental system. The activation energy for barite-NaCl isotope exchange is 13.4 kcal mol^{-1} whereas barite-NaCl plus H_2SO_4 yields a value of 9.2 kcal mol^{-1}.

Summary of oxygen isotopic rate constants

An Arrhenius plot of many of the experimentally determined oxygen isotopic rate lines for dissolution-redeposition is given in Fig. 4. Only those reactions that exhibited new mineral growth or recrystallization are given in this plot. A closer examination of this figure indicates that for specific temperature ranges, rates of oxygen isotopic exchange can be ranked, if we assume that similar conditions prevail for all phases (i.e. W, S, A, t). In general, the following ranking of rates is observed for temperatures between 150 and 350°C.

Strontianite ≈ witherite > barite ≥ calcite ≥ dolomite > sanidine > quartz ≥ albite > kaolinite > paragonite

Above 350°C, ranking becomes more difficult because of the convergence of many of the rate lines. Nevertheless, an approximate order can be given

witherite > strontianite > barite ≥ albite > sanidine > dolomite ≥ calcite ≥ celsian > quartz ≥ kaolinite ≥ paragonite

With the exception of barite and paragonite, the decrease in rate constants exhibited by these phases follows approximately the trend in minerals of increasing tendency to concentrate ^{18}O (O'Neil, 1979). In

fact, the carbonates follow this scheme almost exactly. In general, these relations are observed because bonds formed by the light isotope (^{16}O) are more readily broken than bonds involving the heavy isotope (^{18}O). Thus, during chemical reactions, molecules bearing the light isotope (carbonates, sulfates) will react slightly more readily than those with the heavy isotope (quartz, feldspars, clays).

Because the chemical reactions modeled isotopically in Fig. 4 involved growth of new phases at the expense of reactants or the recrystallization of reactants, isotopic exchange rates should depend on chemical rates of precipitation or dissolution. Berner (1978) points out that interface detachment, not diffusion, is rate controlling over a wide range of measured dissolution rates. Rates of dissolution (k_+) in gm $cm^{-2}sec^{-1}$ for feldspars, quartz and biotite (annite) have been summarized by Norton and Taylor (1979) for temperatures ranging from about 50 to 400°C. Using these rates along with equilibrium constants for the various reactions, the rates of precipitation (k_-) can be estimated from the following

$$\frac{k_+}{k_-} = K \tag{38}$$

$$k_- = \frac{k_+}{K} \tag{39}$$

The equilibrium constants for the dissociation of these phases are derived from Helgeson et al. (1978).

Rate constants for precipitation of K-feldspar, albite, annite and quartz recast in units of moles $m^{-2}sec^{-1}$ are plotted in Fig. 5.

It is apparent that below a temperature of approximately 200°C, the order in rates of precipitation is strikingly similar to the order of oxygen isotopic exchange described above for similar phases. Feldspars precipitate the fastest, followed by quartz and finally annite. Unpublished data from Capuano (1977) indicate that at low temperatures (>100°C) calcite precipitation rates exceed all of these phases (e.g. at 25°C, $k_- = 10^{5.5}$ moles $m^{-2}sec^{-1}$). This lends further credence to our contention that precipitation and/or dissolution rates are directly involved in controlling rates of experimental isotopic exchange, particularly if the rate line of carbonate precipitation has a slope similar to the other phases (see Fig. 5). There is no a priori reason, however, to believe that the rate of precipitation and rate of isotopic exchange controlled by surface exchange should be the same. Indeed, studies of natural systems exhibiting alteration have taught us that chemical equilibrium is closely approached or attained, whereas isotopic disequilibrium between solids and fluids is commonplace. It is important to point out however, that activation energies given for dissolution-precipitation reactions (Lasaga, 1981) are in close agreement to those calculated here for surface-controlled oxygen isotopic exchange.

DIFFUSION-CONTROLLED OXYGEN ISOTOPIC EXCHANGE

Previous work and problems

Most of the experiments designed specifically to measure rates of isotopic exchange have addressed only the diffusional mechanism. These experiments can be divided into two types, hydrothermal and

anhydrous. In the hydrothermal experiments, solids are reacted either with pure water (Giletti et al., 1978) or a salt solution in equilibrium with the solid (Yund and Anderson, 1974). Anhydrous experiments involve the reaction of a solid with either CO_2 or O_2 gas (Muehlenbachs and Kushiro, 1974). Phases that have received the most attention are feldspars, olivine, phlogopite, quartz and magnetite. Table 3 summarizes Arrhenius relations for diffusion of oxygen or oxygen-bearing species in silicates and oxides. For a more complete compilation of diffusion data for a variety of elements (e.g. O, Sr, Na, K) in silicates refer to Hart (1981). We will restrict any further discussion of diffusion to hydrothermal systems (e.g. feldspar-fluid, phlogopite-fluid).

In hydrothermal experiments where chemical equilibrium was established between an aqueous KCl solution and K-feldspar, Yund and Anderson (1974) concluded that volume diffusion of oxygen was the most effective process in the isotopic exchange of oxygen. The isotopic exchange process occurred only in response to difference in the chemical potential of ^{18}O in the aqueous and solid phases. Further experimentation on the effect of fluid pressure on oxygen isotopic exchange between K-feldspar and 2M KCl solution (Yund and Anderson, 1978) produced diffusion coefficients with a positive dependence on fluid pressure. This is opposite from the effect predicted on the basis of oxygen volume diffusion theory. Thus, Yund and Anderson (1978) concluded that oxygen isotopic exchange resulted from diffusion of OH^- or possibly H_2O into the feldspar and not volume diffusion of

oxygen.

However, an isotopic exchange mechanism based on volume diffusion of oxygen was proposed by Giletti and Anderson (1975) and Giletti et al. (1978) for hydrothermal experiments involving phlogopite (4% annite) and feldspars, respectively. Diffusion coefficients obtained from phlogopite-alkali salt solution experiments agreed with those obtained from phlogopite-pure water (Giletti and Anderson, 1975). In addition, oxygen diffusion data determined by Giletti et al. (1978) for K-feldspar-pure water experiments are in good agreement with oxygen diffusion data from K-feldspar-KCl experiments of Yund and Anderson (1974) and Merigoux (1968). The transport data for oxygen (or oxygen-bearing species?) in feldspars indicate that grains may be treated as ideal spheres when calculating diffusion coefficients (Giletti et al., 1978), whereas major oxygen transport in phlogopite occurs across mica layers, parallel to the c-axis (Giletti and Anderson, 1978).

A more detailed discussion of the mechanisms of exchange and problems in the experimental data base for diffusion is given by Norton and Taylor (1979). They believe that all of the hydrothermal experiments described in the literature (diffusion or otherwise) that address isotopic exchange are comprised of incongruent reactions. Specifically, hydrothermal reactions involving calcium-rich plagioclase (An_{96}) and pure water at 350°C and 1kb are out of chemical, as well as isotopic equilibrium. Data plotted in Fig. 2b of Giletti et al. (1978) support this conclusion. In their figure, one can observe

a rapid change in $^{18}O/^{16}O$ ratios in plagioclase (An_{96}) with depth to approximately 1000 Å, after which the ratios remain relatively constant (original plagioclase). This type of profile might be expected for a situation where new mineral growth has occurred in the outer 1μ of the grain. Conversely, volume or bulk-diffusion should produce a smoother, gradually curving profile as exhibited by their Fig. 2a for adularia-pure water interaction. Unfortunately, lack of detailed SEM or x-ray diffraction data on run products precludes the possibility of verifying such contentions.

Certainly, dissolution-redeposition in angstrom-thick layers on surfaces is undoubtedly occurring in many hydrothermal experiments. Yund and Anderson (1974) observed, however, large oxygen isotopic fractions of exchange (0.10 to 0.50), but could detect no structural reordering or recrystallization in K-feldspars reacted with either pure water or KCl solutions below 700°C. Surman and Castle (1969) observed no secondary iron-oxyhydroxides or other phases in hydrothermal experiments involving magnetite and water. They did notice, however, the positive dependency of diffusion on fluid pressure also observed by Yund and Anderson (1978) for K-feldspars. Simple mass balance considerations suggest that large fractions of oxygen isotopic exchange should result from significant recrystallization or deposition, if these mechanisms are indeed controlling exchange. These observations, coupled with the close agreement between oxygen diffusion coefficients calculated from a variety of different feldspar-fluid experiments seem to support the hypothesis that diffusion of

some oxygen-bearing species into solids is probably the dominant mechanism in these so called "diffusion" experiments. Therefore, we will use diffusion coefficients derived from Arrhenius relations given in Table 3 for modeling diffusion-controlled isotopic exchange in mineral-fluid systems.

Diffusion mathematics as applied to isotopic exchange

Diffusion is a process by which the molecules, atoms, or ions, driven by a chemical potential gradient, move from point to point in either a single phase or between two different phases, such as a gas and liquid. When two or more isotopes of a specific element are transferred by a process of diffusion, a change in isotopic abundance ratio would be expected because of the velocity differences of isotopes of a given element. In the case of isotopic exchange during mineral-fluid interaction we need to consider a system in which isotopic fractionation occurs when a solute (oxygen-bearing species) is taken up by the solid. The rate of uptake of the solute and the subsequent isotopic exchange are governed by temperature and the size and shape of the solid.

In addition, Carman and Haul (1954) and Crank (1975) have pointed out that the volumes of solution and solid are also critical in quantifying the rate of equilibration of a given chemical component between two phases. The importance of this volume effect has heretofore been ignored in the application of diffusion coefficient data to the modeling of both hypothetical and natural mineral-fluid systems. For example, Giletti et al. (1978) demonstrated the effects of varying

grain size and temperature on the degree of isotopic equilibration (F) for feldspars, but failed to address the volumes of either solution or feldspar. Because they assumed a constant isotopic composition for the fluid, the examples they give are only valid for a system where the volume of solution greatly exceeds that of the feldspar (or very high water/solid mass ratio).

If, however, we consider a limited volume of solution, the concentration of solute (oxygen-bearing species?) in the solution falls as solute enters the solid. For a solution that is well mixed, the concentration in the solution depends only on time, and is determined essentially by the condition that the total amount of solute in the system (solution plus solid) remains constant as diffusion proceeds (Crank, 1975). From a geologic perspective, it is more appropriate to consider systems where the volume of solution to volume of solid ratio is near unity, give or take an order of magnitude. This is particularly true in hydrothermal and metamorphic systems where small quantities of fluids can occur in microfractures or along grain boundaries.

The following set of equations demonstrates the interrelationships between the various parameters (e.g., temperature, grain size, shapes, volumes) that control isotopic exchange resulting from diffusion of a solute between a solution of limited volume and a solid. Let us first consider the diffusion of a solute from a well-mixed solution of limited volume into a sphere. Suppose that the sphere occupies the space, V_S, whereas the volume of the solution (excluding

the space occupied by the sphere) is V_w. It is assumed that the concentration of solute in solution is always uniform and is initially C_o. The sphere is initially free from solute. The surface of the sphere adjusts to the partition of solute in the following manner

$$(C_2)_s = K'(C_2)_w(t) \tag{40}$$

where $(C_2)_w(t)$ equals the concentration of ^{18}O in the liquid at time t, (C_2) is the ^{18}O concentration in the solid at t and K' is the equilibrium partition ratio corrected for concentration (we will return to this parameter later). The total amount of solute in the sphere after time t is expressed as a fraction (F) of the corresponding quantity after infinite time (equilibrium) by the relation given in Crank (1975).

$$F = 1 - \sum_{n-1}^{\infty} \frac{6\beta(\beta+1)e^{-Dq_n^2 t/a^2}}{9 + 9\beta + q_n^2\beta^2} \tag{41}$$

where the q_n's are the non-zero roots of

$$\tan q_n = \frac{3q_n}{3 + \beta q^2_n} \tag{42}$$

and

$$\beta = \frac{V_w}{V_s K'} \tag{43}$$

or

$$\beta = \frac{3V_w}{4\pi a^3 K'} \tag{44}$$

Because isotopic fractionation occurs during solute uptake into the solid, the fraction of isotopic exchange is equal to the fraction of solute in the solid. Expression (41) is valid for large values of t and demonstrates that the rate of isotopic exchange toward equilibrium (F) is a function of the solution to solid volume ratio β), as well as the grain radius, time and temperature, which fixes D. The roots of equation (42) are given in Table 6.1 of Crank (1975) for several values of β.

If we consider a plane sheet or plate (i.e. mica, clay) suspended in a limited volume of well-mixed solution, an expression for diffusion at long times similar to equation (41) is given

$$F = 1 - \sum_{n=1}^{\infty} \frac{2\beta(1+\beta)\, e^{-Dq_n^2 t/w^2}}{1 + \beta + \beta^2 q_n^2} \qquad (45)$$

where the q_n's are the non-zero roots of

$$\tan q_n = -\beta q_n \qquad (46)$$

and

$$\beta = \frac{V_w}{bwhK^T} \qquad (47)$$

Note that the form of equation (54) is nearly identical to equation (41) for a sphere except that grain radius (a) is replaced by plate thickness (w).

From these diffusion equations (i.e. 41, 45) it is obvious that the fraction of isotopic exchange in systems of limited solution

volume is a function of the same parameters regardless of grain geometry. Once it can be established what grain geometry is best suited for a given mineral, then only the grain size, the volumes of solution and solid, and temperature are required to solve for F. For phases such as feldspars, quartz, magnetite and olivine, a spherical geometry is most appropriate. Hydrous silicates such as phlogopite, muscovite, montmorillonite, and kaolinite are best modeled from a plate geometry.

Of the parameters needed to solve for F, the one that has received the least attention is the solution to solid volume ratio (@). In addition, it is not clear whether volume ratios used to model experimental systems described in the literature have been corrected by use of the equilibrium concentration partition ratio (K'). Because diffusion involves changes in concentration over given distances, the isotopic equilibrium fractionation factor (α_{sw}) can not be substituted directly for K'. Instead, α must be recast into a concentration ratio (K'), that is estimated by taking the ratio of moles of ^{18}O cc^{-1} of solid to moles of ^{18}O cc^{-1} in solution at equilibrium. This is accomplished by selecting an arbitrary $^{18}O/^{16}O$ ratio for the solid, calculating the number of moles of ^{18}O cc^{-1} based on density of the solid, using α_{sw} to estimte an $^{18}O/^{16}O$ ratio for the solution, correcting that for moles of ^{18}O cc^{-1} using the solution density, and finally taking the ratios of these concentrations.

Table 4 gives values of K' for a variety of mineral-water pairs for temperature between 200 and 400°C. The values at any given temperature are remarkably similar for the pairs given because the

densities and moles of oxygen per gram of solid are very similar. The K' values increase with temperature principally because the density of water decreases. If the density was held constant, the K' values for a given mineral-water pair would be nearly identical. Above the critical point of water (>374°C), the critical density of water (~0.3156 gm cc^{-1}) was used in the calculations. Application of K' values in the equations that solve for β (e.g. equation 43) results in the conversion of β to a mass ratio, and hence it can be known as a corrected water/solid ratio. Therefore, if the diffusion equations given above are adhered to rigorously, the change in isotopic exchange toward equilibrium can be modeled for various temperatures, grain sizes and shapes, and water/solid ratios.

The calculation of (F) for given values of (D), (a) or (w) and (t) is readily accomplished by solving equations (41) and (45) graphically (Fig. 6a and 6b). In these figures modified form Crank (1975), the fraction of isotopic exchange is plotted against either Dt/a^2 for a sphere (Fig. 6a) or Dt/w^2 for a plate (Fig. 6b). The contours shown on these figures represent the percentage of total solute finally taken up by the solid, where

$$\% = \frac{1}{1 + \beta} \quad 100 \qquad (48)$$

By knowing the solution to solid volume ratio (β), the diffusion coefficient (D), grain size (a or w), and grain geometry (sphere or plate), the fraction of isotopic exchange (F) can be determined for any time (t). Figs. 6a and 6b are useful only for systems where a

solid is interacted with a well-mixed solution of limited volume.

COMPARISON OF SURFACE EXCHANGE AND DIFFUSION MODELS

Rate of oxygen isotopic equilibration for the surface exchange process

In a previous section, we gave an equation (36) that solved for the time required to attain a certain fraction of isotopic exchange as a function of surface area, temperature and the number of moles of oxygen in the solid and solution. Before a direct comparison can be made with diffusion-controlled isotopic exchange modeled in Figs. 6a and 6b, the isotopic rate equation (31) for surface exchange must be modified. This can be accomplished by rearrangement of the A, W and S terms which are interrelated.

For a spherical grain, the surface area (A) can be represented by

$$A = 4\pi(a^2) \cdot N \tag{49}$$

where (a) is the average grain radius (cm) and N is the number of particles given by

$$N = \frac{3M_S}{\rho 4\pi(a)^3} \tag{50}$$

with the mass of the solid (in gm) and its density (gm cc^{-1}) represented by M_S and ρ, respectively. By converting M_S to moles of oxygen and factoring, A in equation (49) is transformed to

$$A = \frac{3S}{(X_S)\rho a} \tag{51}$$

where S is the total number of moles of oxygen in the solid and X_S is

the average number of moles of oxygen per gram of solid. Substituting (51) into equation (31) yields

$$r_1 = \frac{-\ell n(1-F)(WS)(X_s)(a)(\rho)}{3S(W+S)t} \qquad (52)$$

which, upon rearrangement of terms, converts to

$$r_1 = \frac{-\ell n(1-F)(W/S)(X_s)(a)(\rho)}{3(1+W/S)(t)(10^{-4})} \qquad (53)$$

where (W/S) is the mole ratio of oxygen in water to solid. The term, 10^{-4} is needed to convert from cm^2 to m^2. By rearranging equation (53), the time required to attain a given fraction of isotopic exchange (F) can be evaluated for different temperatures, water/solid ratios and grain sizes as follows

$$t = \frac{-\ell n(1-F)(W/S)(X_s)(a)(\rho)}{3(1+W/S)(r_1)(10^{-4})} \qquad (54)$$

A similar expression is derived for a grain with an octagonal plate geometry

$$t = \frac{-\ell n(1-F)(W/S)(X_s)(w)(\rho)}{(1+W/S)(r_1)(10^{-4})} \qquad (55)$$

where the plate thickness (w) is used in place of grain radius. These two expressions (54 and 55) and the ones for diffusion of a solute into a sphere (41) or a plate (45) modeled graphically can now be used to compute the change in the fraction of isotopic exchange toward

equilibrium with time for a system with a specified temperature, water/solid mass ratio, grain size and grain density.

Oxygen isotopic exchange in hypothetical mineral-fluid systems

In order to illustrate the differences and similarities between the surface exchange and diffusion models, we will examine the interaction of feldspars and micas with fluids. These phases are particularly important because of their ubiquitous occurrence in natural environments. In addition, most of our knowledge concerning mechanisms and rates of isotopic exchange are derived from experiments on feldspars and micas.

The results of model calculations are graphically depicted in Figs. 7-10. Figures 7 and 8 show the fraction of isotopic exchange represented as $\ell n(1-F)$ plotted against time in years. Oxygen isotopic exchange by means of diffusion in the systems albite-water and phlogopite-water was modeled for 300 and 400°C, grain sizes of 0.01, 0.1 and 1.0 cm and varying fluid/mineral mass ratios (0.1, 1.0 and 10). Similarly, surface-controlled isotopic exchange was modeled for albite altering to K-feldspar and paragonite altering to muscovite and 300 and 400°C, with variable grain sizes and fluid/mineral mass ratios. The fluid/mineral mass ratio is readily converted to volume ratio for use in Figs. 6a and 6b or as the oxygen mole ratio used in equations (54) and (55). For example, a fluid/albite mass ratio of one is equal to an oxygen mole ratio of 1.82 or a volume ratio of 2.62. It is important to reiterate that the volume ratios used in the diffusion equations must be corrected for concentration by use of the

equilibrium partition ratios (K') given in Table 4.

Results of the surface exchange calculations plotted in the upper portions of Figs. 7 and 8 indicate that the time required to attain a certain fraction of exchange is less for lower fluid/mineral mass ratios. For example, a 0.01 cm albite grain altered to K-feldspar at 400°C reaches 90% exchange in 0.17 years for a fluid/mineral mass ratio of 1.0, but only 0.04 years with a mass ratio of 0.1 (Fig. 7). A similar decrease in time is observed for paragonite altering to muscovite as the fluid/mineral mass ratio is decreased (Figs. 7, 8). Because of the divergent nature of the straight lines, this difference in time continually increases with increasing fraction of exchange.

An increase in the grain size produces a similar result, where the time to achieve a given fraction of exchange increases. At a constant fluid/mineral mass ratio of 0.1, the time required to reach 50% exchange for albite reacted to K-feldspar at 300°C (Fig. 8) increases from .05 to over 32 years as a consequence of increasing the grain size from 0.01 to 1 cm. A change in grain thickness of 0.001 to 0.1 cm for paragonite reacted to muscovite at 300°C results in an increase in time to attain 50% exchange from 5 years to over 350 years, at a constant fluid/mineral mass ratio of 0.1. These increases in time corresponding to changes in the grain size are greater than the time differences resulting from increases of comparable magnitude in the fluid/mineral mass ratio.

Diffusion-controlled isotopic exchange shown in the lower portions of Figs. 7 and 8 behaves in a manner similar to surface

exchange. The time required to attain a given fraction of exchange increases with an increase in either grain size or fluid/mineral mass ratio. The times for diffusion exchange, however, are several orders of magnitude slower than surface exchange. A system at 400°C with a grain radius of 0.01 cm and a fluid/mineral mass ratio of one reaches 90% exchange in about 0.17 years for albite altering to K-feldspar versus 800 years for oxygen diffusion in albite (Fig. 7c). Another significant difference is in the shape of the curves. Straight lines are produced for the surface exchange model, whereas curves exhibiting a less rapid increase in fraction of exchange with increase in time are observed for the diffusion model. The curves calculated for diffusion do, however, mimic the straight lines for surface exchange in that they diverge with increasing time.

In dynamic geologic systems, parameters that influence isotopic exchange such as temperature and fluid/mineral mass ratios may also undergo change as the systems evolve toward equilibrium. The rate of equilibration of various mineral-fluid systems can be conveniently portrayed by expressing the time in years to achieve a certain degree of equilibrium as a function of the temperature (Fig. 9) or the fluid/mineral mass ratio (Fig. 10). Figure 8 demonstrates the obvious, that the time required to achieve equilibrium increases with decreasing temperature. This figure also shows that depending on the temperature, one phase may exchange faster than another. For example, at 400°C, albite altering to K-feldspar generally exchanges isotopes more readily than either quartz recrystallization or paragonite

conversion to muscovite, under similar grain size and (W/S) conditions (Fig. 9). Below 300°C, however, quartz recrystallization and, in limited cases, paragonite alteration to muscovite approach equilibrium faster. In the case of diffusion (Fig. 9), feldspars tend to equilibrate faster than phlogopite at all temperatures for comparable grain size and (W/S) conditions.

Interestingly, Figure 10 demonstrates a characteristic common to both surface exchange and diffusion. This figure shows that as the fluid/mineral mass ratio increases the rate of change in the times required to attain 90% exchange decreases. Therefore, the times required to attain 90% exchange at a (W/S) = 10^4 is not much greater than that calculated for a (W/S) = 10. The most significant effects on time resulting from changes in fluid/mineral mass ratios are observed for values less than about 0.001. Times change quite radically in the region of (W/S) less than 0.001 as the curves approach the ordinate axis asympototically. In general, an increase in time of approximately one order of magnitude occurs when the fluid/mineral mass ratio is increased from 0.1 to 10. This (W/S) range is thought to be typical of values exhibited by many continental hydrothermal ore deposits and metamorphic terrains (Taylor, 1979).

CONCLUSIONS

Isotopic exchange accompanying the interaction of minerals and fluids is controlled by one of two major mechanisms, surface exchange or diffusion. Surface exchange is controlled dominately by dissolution-reprecipitation or recrystallization reactions.

Diffusion, on the other hand, involves transport of an oxygen (hydrogen)-bearing species through phases either along lattice planes or crystal imperfections. Each of these mechanisms is in turn, controlled by a common set of physical and chemical parameters that we have evaluated quantitatively.

The rate constant for isotopic exchange accompanying surface reactions was shown to be proportional to the degree of equilibrium and the product of the number of moles of oxygen (or hydrogen) in solution and solid, and inversely proportional to the surface area, the total moles of oxygen (hydrogen) in the system and time. Estimates of rate constants obtained from experimental data on oxygen isotopic exchange reactions fall between approximately 10^{-4} and 10^{-8} moles $m^{-2}sec^{-1}$, with activation energies ranging from about 8 to 22 kcal mol^{-1}. In general, oxygen isotopes are exchanged fastest by carbonates, followed by sulfates and finally silicates. The rate constants calculated for individual silicate-water systems are comparable to those determined from the bulk rock (granite, basalt) - fluid experiments of Cole (1980).

By rearranging the isotopic rate equation for surface exchange, the time required to attain a given degree of equilibrium can be evaluated as a function of grain size, grain density, grain geometry, water/solid mass ratio and rate at a particular temperature. Similarly, expressions were found that relate the diffusion coefficient, grain size, grain geometry, water/solid mass ratio and time to the fraction of isotopic exchange resulting from diffusion. Calculations

using the surface exchange and diffusion equations indicate that the time required to attain isotopic equilibrium increases with an increase in either the water/solid mass ratio and/or grain size, or a decrease in temperature. The principal difference being, however, that rates of exchange involving surface reactions are orders of magnitude faster than isotopic exchange accompanying diffusion.

The calculations discussed above demonstrate that systems experiencing surface-controlled isotopic exchange reach equilibrium well before diffusion-controlled isotopic exchange can become a significant contributor. The extent to which surface alteration influences the overall isotopic exchange of a solid depends on the abundance of the reaction product(s) and its mineralogy (Cole, 1980). In situations where alteration of a solid is not complete, the remaining isotopic exchange is accomplished by diffusion of an oxygen-bearing species into the unaltered portion of the grain. Final isoopic equilibrium may be achieved in periods as short as a few months for phases altered completely to secondary minrals, or in excess of 10^6 years for systems exchanging entirely by diffusion. As long as both processes are not in competition, systems influenced by both should exhibit equilibration times similar to the slower process, diffusion.

The significant difference in rates of equilibration observed between the two mechanisms suggests that they may be mutually exclusive in natural systems. For example, oxygen isotopic shifts observed in hydrothermal ore deposit and geothermal systems have been

shown to be the result of alteration reactions during rock-water interaction (Taylor, 1979). In higher temperature igneous and metamorphic systems, isotopic exchange resulting from initial crystallization of phases is commonly erased by later retrograde processes dominated by diffusion of oxygen-bearing species from thin fluid films into solids (Bottinga and Javoy, 1975). In lower temperature environments (<100°C), Yeh and Savin (1976) attributed partial oxygen isotopic exchange between clays and seawater to crystallization reactions, whereas Lawrence and Kastner (1975) demonstrated that oxygen isotopic exchange observed in detrital feldspars contained in carbonates resulted from diffusion.

Application of surface exchange and diffusion equations to well-studied geologic systems should prove useful in quantifying either time or water/solid mass ratios regardless of the degree of equilibrium. These estimates can then be tested by more rigorous mass transfer and fluid flow modeling.

APPLICATIONS

The calculations discussed above demonstrate that systems experiencing surface-controlled isotopic exchange reach equilibrium well before diffusion-controlled isotopic exchange can become a siginificant contributor. The extent to which surface alteration influences the overall isotopic exchange of a solid depends on the abundance of the reaction product (s) and its mineralogy (Cole, 1980). In situations where alteration of a solid is not complete, the remaining isotopic exchange is accomplished by diffusion of an oxygen-bearing species into the unaltered portion of the grain. Final isotopic equilibrium may be achieved in periods as short as a few months for phases altered completely to secondary minerals, or in excess of 10^6 years for systems exchanging entirely by diffusion. As long as both processes are not in competition, systems influenced by both should exhibit equilibration times similar to the slower process, diffusion.

The significant difference in rates of equilibration observed between the two mechanisms suggests that they may be mutually exclusive in natural systems. For example, oxygen isotopic shifts observed in hydrothermal ore deposit and geothermal systems have been shown to be the result of alteration reactions during rock-water interaction (Taylor, 1979). In higher temperature igneous and metamorphic systems, isotopic exchange resulting from initial crystallization of phases is commonly erased by later retrograde processes dominated by diffusion of oxygen-bearing species from thin fluid films

into solids (Bottinga and Javoy, 1975). In lower temperature environments (<100°C), Yeh and Savin (1976) attributed partial oxygen isotopic exchange between clays and seawater to crystallization reactions, whereas Lawrence and Kastner (1975) demonstrated that oxygen isotopic exchange observed in detrital feldspars contained in carbonates resulted from diffusion.

Application of the surface exchange and diffusion equations to these and other examples are illustrated below. No attempt has been made to integrate these rate equations with mass transfer and fluid flow models. A later paper in this series will address the applications of this type of modeling to various geologic systems. Instead, our aim in this section is to quantify one or more of the parameters (time, W/S, grain size) that have influenced isotopic exchange in a variety of geologic systems.

Time estimates for mineral-fluid interaction in various geologic systems

Hypothetical examples have been given (see Figs. 7 and 8) that demonstrate that time of mineral-fluid interaction can be calculated for systems controlled by either a surface exchange or diffusion mechanism. All that is required is a knowledge of temperature, grain size, grain geometry, water/solid mass ratio, and degree of equilibration. A few environments have been selected to illustrate how natural data can be applied to either surface exchange (54, 55) or diffusion equations (41, 45) to model time. These systems are listed in Table 5 along with a summary of values used in the rate equations.

Temperature data for hydrothermal systems are derived from either direct measurements (Wairakei, Salton Sea) or fluid inclusion filling temperatures (Creede). A bottom ocean temperature of 1°C was selected for North Pacific sediments (Yeh and Savin, 1976). A diagenetic temperature of approximately 50°C was assumed for feldspar-bearing carbonates at Glacier Park, Montana and Madoc, Ontario (Lawrence and Kastner, 1975). Values for grain sizes (cm) were derived from descriptions of rock units in the various systems. We have assumed that the solid-fluid interactions occurred under conditions of constant temperature and grain size, and that the fluid flow rates were slower relative to chemical or isotopic exchange rates, such that the systems appear static.

If possible, the fluid/solid mole ratios were estimated from the following equation

$$\frac{W}{S} = \frac{\delta_s^i - \delta_s^f}{\delta_w^f - \delta_w^i} \qquad (56)$$

where δ is the isotopic composition of a phase, i and f refer to initial and final, respectively, and w and s represent fluid and solid, respectively. Note that the final isotopic compositions of the fluid and solid need not be equilibrium values to solve for (W/S). In cases where δ_w^i and δ_w^f are not known (i.e. Glacier Park, Madoc), (W/S) values were derived from average porosities of the rocks. Porosity in carbonates averages approximately 13% (Levorsen, 1965). If we assume all voids were filled with fluid, the approximate mole ratio of (W/S) is 0.1.

The degree of equilibration (F) can be computed only if the initial, final and equilibrium value of either the solid or fluid are known. When the fluid and solid become isotopically equilibrated at a given temperature, the equilibrium composition of the fluid (δ_w^{eq}) can be expressed as

$$\delta_w^{eq} = \frac{\delta_s^i - 1000\ \ell n\alpha_{sw} + (W/S)\ \delta_w^i}{1 + (W/S)} \tag{57}$$

and

$$\delta_s^{eq} = 1000\ \ell n\alpha_{sw} = \delta_w^{eq} \tag{58}$$

The fraction of exchange can be calculated from

$$F = \frac{\delta_w^f - \delta_w^i}{\delta_w^{eq} - \delta_w^i} = \frac{\delta_s^i - \delta_s^f}{\delta_s^i - \delta_s^{eq}} \tag{59}$$

for systems where the isotopic compositions of the solid and fluid shift toward one another (i.e. high temperature, small values of $1000\ \ell n\alpha_{sw}$). Conversely, the fraction of exchange in low temperature systems where isotopic shifts commonly occur in opposite directions can be evaluated from

$$F = \frac{\delta_w^i - \delta_w^f}{\delta_w^i - \delta_w^{eq}} = \frac{\delta_s^f - \delta_s^i}{\delta_s^{eq} - \delta_s^i} \tag{60}$$

The consequences of mixing or boiling on fraction of isotopic exchange which are particularly important in hydrothermal systems has not been considered. For a more complete discussion refer to Cole (1980).

The final parameter that is required before implementation of the

surface exchange or diffusion equations is the rate constant of exchange. For hydrothermal systems such as Wairakei, Salton Sea and Creede, surface exchange rate constants are used. Yeh and Savin (1976) argue convincingly that the clays they examined isotopically were formed by recrystallization reactions which resulted from the interaction of sediments and seawater. On the other hand, Lawrence and Kastner (1975) demonstrated that detrital feldspars contained in ancient carbonate beds underwent isotopic exchange through a diffusional mechanism. In the case of these low temperature environments, rate constants or diffusion coefficients from specific mineral-fluid systems can be matched quite closely to the actual natural assemblage (i.e. kaolinite for clays in the North Pacific, adularia for K-feldspar at Glacier Park and Madoc). In the hydrothermal systems, however, phases were selected that most closely approach the composition of the bulk rock undergoing exchange. This assumption is valid because Cole (1980) has shown that rock-water isotopic exchange rates are comparable to rates predicted for separate mineral-fluid systems.

From the values given for these parameters in Table 5, estimates are made of the duration of isotopic exchange observed in the various environments. These times do not represent the age of the deposits, but rather, the duration required to produce the observed isotopic shifts in solids and fluids. The durations of time calculated for diffusion in feldspars are somewhat less than the ages of the sediments implying that the diffusion process may have been more or less continuous since the time of deposition. Conversely, the time

estimated for isotopic exchange observed in clay sediments from the North Pacific appears to be much shorter compared to the proposed age of deposition (>14,000 years).

Hydrothermal systems influenced predominately by surface exchange reactions exhibit a more restricted range in times compared to the low temperature environments. These times range from 40 years for the Salton Sea to as much as 700 years for Wairakei, New Zealand. The total duration of hydrothermal activity in these systems is probably on the order of a few thousand to tens of thousands of years (Barnes, 1979). For example, Barton et al. (1977) estimate a time of approximately 2000 years was required for ore deposition at Creede. Therefore, the times estimated by the surface exchange model may represent only single episodes in the lifetime of these systems. Additional field-related criteria are needed to quantify the number of episodes so that ages can be estimated.

Influence of grain size variations on isotopic exchange

The oxygen isotopic systematics in many Teritary igneous systems have been explained on the basis of the grain size of phases within various igneous units (Forester and Taylor, 1977, 1980). Isotopic exchange in these systems probably took place at subsolidus temperatures ranging from 300 to 550°C. Commonly, increases in isotopic depletion of ^{18}O in plagioclase correlate with the decrease in average grain size (see Fig. 7 of Forester and Taylor, 1980). These isotopic depletions are the result of preferential recrystallization along cracks and imperfections as well as diffusion of oxygen-bearing

species through portions of the unaltered plagioclase lattice (Taylor, 1974). Final equilibration was controlled by the slower of the processes, diffusion.

From the diffusion modeling for spheres (see Fig. 6a) discussed previously, we can illustrate why data plotted on Forester and Taylor's (1980) Fig. 7 should take the shape of a Z. The results of these computations are given in Fig. 11. We have assumed that isotopic exchange occurs by a diffusional process at 300°C in anorthite whose initial $\delta^{18}O$ composition is +7.5°/oo. We further assume this interaction occurs at a constant fluid/mineral mass ratio of 0.2 as suggested by Forester and Taylor (1980) for the Stony Mountain Complex, Colorado. The final equilibration value for plagioclase in such a system is approximately 2.4°/oo, or a depletion value of 5.1%.

Not too surprisingly, the shape of curves given in Fig. 11 duplicates exactly the shape of a curve fit to data given by Forester and Taylor (1978). Specifically, their data appear to conform to a set of curves shown on Fig. 11 that were calculated for times in excess of 10,000 years. This, of course, is an over simplification because temperatures and (W/S) ratios could vary from sample to sample. In any event, these curves approach the $\delta^{18}O$ depletion value for equilibrium (5.1°/oo) asymptotically with decreasing grain radius. Conversely, as grain radii exceed 0.5 to 1.0 cm, anorthite exhibits less than 0.5°/oo depletion for times ranging from 100 to 50,000 years. We believe that with more detailed information on temperatures, grain sizes and probable (W/S) ratios, similar modeling

could put constraints on the duration of isotopic exchange in subsolidus igneous systems. These values could then be tested by more rigorous mass transfer and fluid flow modeling (see Norton and Taylor, 1979 for the best example).

Diffusion effects on attainment of isotopic equilibrium between mineral pairs

Isotopic disequilibrium observed in some metamorphic systems is similar in many respects to isotopic disequilibrium discussed above for subsolidus igneous environments. In general, however, retrograde processes used to explain disequilibrium in metamorphism result from interaction of evolved fluids (e.g. previously meteoric, seawater or connate water) with rocks rather than the influx of pristine meteoric water as postulated for Tertiary igneous complexes (Taylor, 1979). Recrystallization and/or nucleation of new phases is probably rapid at temperatures greater than 300°C, as demonstrated by Martin and Fyfe (1970). They showed that reactions such as hydration of olivine at temperatures above 200°C proceed to 90% completion in less than two months depending on the (W/S) mass ratio. Since we know that isotopic exchange accompanying recrystallization is very rapid, retrograde processes probably involve diffusion of oxygen-bearing species from thin fluid films into grains that have been involved in an earlier recrystallization event.

One criteria that has been employed to demonstrate disequilibrium is the oxygen isotope partitioning among contemporaneous minerals such as feldspars and mica in igneous and metamorphic rocks. Bottinga and

Javoy (1975) have discussed in detail the use of mineral-pair fractionation factors for estimating either equilibrium temperatures or the extent of disequilibrium in various mineral systems. We can show through the use of Figs. 6a and 6b for diffusion in a sphere (feldspars) and for a plate (mica) respectively, that mineral pair fractionation factors are misleading in terms of estimating equilibrium temperatures or demonstrating disequilibrium.

We have selected the mineral pair albite-phlogopite because of the availability of useful diffusion coefficients (Table 3). The results of calculations on a 400°C system with a mole ratio of fluid to solid of one and grain sizes of 0.05 and 0.005 cm for albite (radius) and phlogopite (thickness) are given in Fig. 12. This figure shows that the oxygen isotopic fractionation between the pair exhibits equilibrium values (0.72‰) at least twice in the exchange history, once at about 100 years and a second at approximately 2×10^6 years. This second time represents the true equilibration time for the pair. Depending on the relative magnitude of the diffusion coefficients and grain sizes, the first cross-over could occur at various times depending on the mineral pair used. Therefore, one could never be positive that the fractionation measured represented equilibrium. In addition, because there is no unique fractionation value, except at the bottom of the trough plotted in Fig. 12, the degree of isotopic equilibrium (F) derived from this type of data is useless in any attempt to quantify the time of interaction. Perhaps a more useful technique in quantifying disequilibrium in metamorphic systems would

be to examine a single phase, such as feldspar and map out $^{18}O/^{16}O$ gradients by using the ion microprobe in a manner similar to that described by Giletti et al. (1978).

Isotopic exchange between a fluid and a hypothetical mica quartz monzonite

In all of the systems discussed thus far, we have applied rate constants or diffusion coefficients from individual mineral-fluid systems to natural environments that involve fluid interaction with a hetrogeneous solid. Pore fluids in sediments, inclusion fluids from ore deposits, hot spring waters, and thin fluid films in metamorphic settings all represent solutions that have reacted with many phases during the course of their chemical and isotopic evolution. It is critical for us to understand the rates of bulk rock-fluid isotopic exchange as well as rates for individual reactions.

Figure 13 illustrates how individual mineral-fluid isotopic rate data can be combined to produce fraction of exchange versus time plots. In this example, a hypothetical rock with albite (X_{ab} = 0.5), K-feldspar (X_{ksp} = 0.15), quartz (X_{qtz} = 0.25) and paragonite (X_{p} = 0.1) was reacted with an aqueous fluid at various temperatures (200-350°C) and times, at a constant (W/S) mass ratio of 0.5. Rate constants for surface exchange were derived by weighting each individual mineral-fluid Arrhenius relation (Table 2) according to mineral abundance and summing over all of these to produce a bulk rock-fluid relation

$$\log_{Rock\text{-}Water} = 3.98\ (1000/T) - 0.83 \qquad (61)$$

Rate constants calculated for temperatures of 200, 250, 300 and 350°C were used in equation (54) to estimate the time required to attain given fractions of isotopic exchange (a spherical grain geometry has been assumed). As expected, the computations yield straight lines on a plot of -ℓn(1-F) versus time (Fig. 3). Note that diffusion modeled for a similar system would appear much like the albite curves in Fig. 8c for 300°C.

The validity of the lines shown in Fig. 3 can only be tested with experimental data. Biotite quartz monzonite-fluid isotopic experimental data (Cole, 1980) have been modeled for 300°C with equation (54) and the results also plotted in Fig. 3. Good agreement is observed between the hypothetical and experimental lines for 300°C. However, the fluids used in the bulk rock experiments were much more dilute (0.1 - 1 m NaCl) compared to solutions used in most of the individual mineral-fluid experiments whose rates we have calculated with equation (31). These data suggest that other types of chemical reactions have occurred in the bulk rock experiments and that isotopic modeling of hypothetical systems is valid only for the reactions given in Table 2. Mineralogic and isotopic data from bulk rock-fluid experimental studies will be presented in other papers in this series.

Table 1. Summary of run conditions used for oxygen isotopic exchange experiments described in the literature.

Source (a)	Temperature Range (°C)	Reactants: Solid	Reactants: Solution	Products (b)	Weights: Solid (gm)	Weights: Solution (gm)	Average Particle Size Range (cm) (c)	Average WS/W+S (d)	Average A(m^2) (c)	Time Range (sec)
O/T67	420-800	Celsian	2m $CaCl_2$	Anorthite	0.025	0.2	0.00075	5.08×10^{-4}	0.00308	4.3×10^{5} - 3.78×10^{6}
O/T67	600	Glass-An	H_2O	Anorthite	0.025	0.2	0.0025	6.75×10^{-4}	0.00362	2.77×10^{5} - 5.18×10^{5}
O/T67	350-800	Sanidine	2-3m NaCl	Albite	0.025	0.2	0.00075 - 0.0055	6.75×10^{-4}	$5.3 - 39.1 \times 10^{-4}$	7.92×10^{4} - 1.89×10^{6}
O/T67	350-650	Albite	3m KCl	K-feldspar	0.025	0.2	0.0025 - 0.0113	7.14×10^{-4}	$5.2 - 11.4 \times 10^{-4}$	3.6×10^{3} - 4.03×10^{6}
O/T67	500-800	Sanidine	H_2O	(Sanidine)	0.025	0.2	0.00075 - 0.0055	6.75×10^{-4}	$5.3 - 39.1 \times 10^{-4}$	1.72×10^{5} - 5.36×10^{5}
O/T67	585-650	Albite	H_2O	(Albite)	0.025	0.2	0.0025	7.14×10^{-4}	1.145×10^{-3}	2.23×10^{5}
O/T69	350-600	Paragonite	3M KCl	Muscovite	0.025	0.2	$(30 \times 24 \times 2.4) \times 10^{-6}$	7.33×10^{-4}	0.0914	1.58×10^{5} - 4.03×10^{6}
C/O/M	195-600	Quartz	0.7m NaF	Quartz	0.0225	0.2	2.5×10^{-5}	7.02×10^{-4}	0.1019	8.6×10^{4} - 4.31×10^{6}
M/G/C	400-700	Quartz	H_2O	(Quartz)	0.01	0.0058	0.0001	1.63×10^{-4}	0.01132	4.32×10^{5} - 1.21×10^{6}
M/G/C	400-700	Albite	H_2O	(Albite)	0.01	0.0058	0.0001	1.56×10^{-4}	0.01145	1.72×10^{5} - 6.05×10^{5}
C/A	305-700	Calcite	H_2O	Calcite	0.035	0.2	$(19 \times 9.5 \times 12) \times 10^{-4}$	9.59×10^{-4}	0.00133	3.96×10^{4} - 4.0×10^{6}
O/C/M	197-493	Calcite	H_2O	Calcite	0.03	0.2	$(64 \times 32 \times 41) \times 10^{-5}$	8.3×10^{-3}	0.00345	1.22×10^{-6} - 1.6×10^{-6}
O/C/M	60-200	Strontianite	0.7m NH_4Cl	Strontianite	0.03	0.2	$(64 \times 32 \times 41) \times 10^{-5}$	5.98×10^{-4}	0.002514	1.58×10^{5} - 5.0×10^{6}
O/C/M	103-205	Witherite	0.7m NH_4Cl	Witherite	0.03	0.2	$(64 \times 32 \times 41) \times 10^{-5}$	4.38×10^{-4}	0.002175	1.58×10^{5} - 6.59×10^{5}
N/C	255-660	Dolomite	0.5m NH_4Cl	Dolomite + Mg Calcite	0.025	0.21	$(14 \times 7 \times 9) \times 10^{-4}$	7.61×10^{-4}	0.00123	3.28×10^{5} - 2.14×10^{6}
O/K	100-350	Kaolinite	0.04N NaCl	Pyrophyllite + Diaspore	0.15	0.5	$(22 \times 11 \times 13) \times 10^{-4}$	4.4×10^{-4}	0.00536	5.7×10^{6} - 5.05×10^{7}
K	170-320	Glass-Kaol.	H_2O	Kaolinite	0.05	0.15	0.001 - 0.01 ?	1.44×10^{-3}	$1.15 - 11.5 \times 10^{-3}$	8.64×10^{5} - 9.24×10^{6}
K	170-320	Glass-Mont.	H_2O	Mont.	0.05	0.15	0.001 - 0.01 ?	1.32×10^{-3}	$1.15 - 11.5 \times 10^{-3}$	1.73×10^{6} - 6.22×10^{6}
K/R	110-350	Barite	1m H_2SO_4 + 1m NaCl	Barite	0.2	10.0	0.0015	3.41×10^{-3}	8.94×10^{-3}	1.1×10^{6} - 1.18×10^{7}
K/R	110-350	Barite	1m NaCl	Barite	0.1	5.0	0.0015	1.70×10^{-3}	4.47×10^{-3}	1.9×10^{6} - 2.97×10^{7}

Notes

(a) O/T67 = O'Neil and Taylor (1967); O/T69 = O'Neil and Taylor (1969); C/O/M = Clayton et al. (1972); M/G/C = Matsuhisa et al. (1979); C/A = Chai and Anderson (1974); O/C/M = O'Neil et al. (1969); N/C = Northrop and Clayton (1966); O/K = O'Neil and Kharaka (1976); K = Kulla (1979); K/R = Kusakabe and Robinson (1977).

(b) Phases formed either as an alteration product of the reactant or as recrystallized reactant. Phases in parenthesis are for experiments where recrystallization and/or alteration were not convincingly demonstrated.

(c) Particle sizes for feldspars, quartz, barite and ground glass are given as radii assuming a spherical geometry. Particle sizes for sheet silicates such as paragonite and kaolinite are given as the base × width × height assuming a octagonal plate geometry. A rhombohedral geometry is assumed for carbonates with particle sizes representing the base × width × height. See the text for a discussion of particle sizes and estimation of surface area.

(d) The ratio of the product of the number of moles of oxygen in water (W) and solid (S) to the sum the number of moles of oxygen in the system.

Table 2. Temperature functions of the oxygen isotopic rate constants for various mineral-fluid reactions.

Reaction: (m)	Data Source	Log r = (k)	r_g (l)	Activation Energy kJ/mol	kcal/mol
1. Sanidine + 3m NaCl = Albite + 3m KCl	a	-3.831(1000/T) - 0.518	-0.91	73.4	17.5
2. Sanidine + H_2O = Sanidine + H_2O	a	-3.767(1000/T) - 1.814	-0.88	72.2	17.2
3. Celsian + 2m $CaCl_2$ = Anorth + 2m $BaCl_2$	a	-4.789(1000/T) - 0.231	-0.99	91.8	21.9
4. Ab + 3m KCl = Ksp + 3m NaCl	a	-5.596(1000/T) + 2.181	-0.90	107.2	25.6
5. Ab + H_2O (NaCl) = Ab + H_2O (NaCl)	a	-4.634(1000/T) - 1.441	-0.88	88.8	21.2
6. Parag. + 3M KCl = Musc. + 3M NaCl	b	-3.225(1000/T) - 3.684	-0.95	61.8	14.8
7. Qtz + 0.7m NaF = Qtz + 0.7m NaF	c	-1.151(1000/T) - 5.893	-0.96	22.1	5.3
8. Qtz + 0.7m NaF = Qtz + 0.7m NaF	c	-1.225(1000/T) - 6.674	-0.91	23.5	5.6
9. Qtz + H_2O = Qtz + H_2O (15kb)	d	-2.368(1000/T) - 4.406	-0.97	45.4	10.8
10. Ab + H_2O = Ab + H_2O (~12kb)	d	-4.424(1000/T) - 1.509	-0.99	84.8	20.2
11. Cc + H_2O = Cc + H_2O	e	-2.273(1000/T) - 3.325	-0.86	43.5	10.4
12. Cc + H_2O (NH_4Cl) = Cc + H_2O (NH_4Cl)	f	-1.375(1000/T) - 4.576	-1.0	26.3	6.3
13. Stron + NH_4Cl = Stron + NH_4Cl	f	-1.389(1000/T) - 2.992	-0.87	26.6	6.4
14. Wither + NH_4Cl = Wither + NH_4Cl	f	-2.219(1000/T) - 1.363	-0.98	42.5	10.2
15. Dol + NH_4Cl = Dol + MgCc + NH_4Cl	g	-2.383(1000/T) - 2.970	-0.93	45.7	10.9
16. Kaol + 0.04N NaCl = Pyroph + Diaspore	h	-2.085(1000/T) - 5.330	-0.97	39.9	9.5
17. Kaol Glass + H_2O → Kaol + H_2O (0.01cm)	i	-1.827(1000/T) - 2.468	-0.92	35.0	8.4
18. Kaol Glass + H_2O → Kaol + H_2O (0.001cm)	i	-1.827(1000/T) - 3.468	-0.92	35.0	8.4
19. Barite + 1m NaCl + 1m H_2SO_4 = Bar + Soln	j	-2.01 (1000/T) - 2.515	-0.97	38.5	9.2
20. Barite + 1m NaCl = Bar + Soln	j	-2.937(1000/T) - 1.323	-0.98	56.3	13.4
21. Mont Glass + H_2O → Mont + H_2O (0.01cm)	i	-3.122(1000/T) - 0.039	-0.99	59.8	14.3
22. Mont Glass + H_2O → Mont + H_2O (0.001cm)	i	-3.122(1000/T) - 1.039	-0.99	59.8	14.3

Notes

Data Source:

(a) O'Neil and Taylor (1967)
(b) O'Neil and Taylor (1969)
(c) Clayton et al. (1972)
(d) Matsuhisa et al. (1979)
(e) Anderson and Chai (1974)
(f) O'Neil et al. (1969)
(g) Northrop and Clayton (1966)
(h) O'Neil and Kharaka (1976)
(i) Kulla (1979)
(j) Kusakabe and Robinson (1977)

(k) Rate constant r in moles O $m^{-2}sec^{-1}$
(l) r_g is the regression coefficient

(m) Abbreviations: Anorth = Anorthite, Ab = Albite, Parag = Paragonite, Musc, = Muscovite, Qtz = Quartz, Cc = Calcite, Stron = Strontianite, Wither = Witherite, Dol = Dolomite, Kaol = Kaolinite, Pyroph = Pyrophyllite, Mont = Montmorillonite, Bar = Barite

Table 3. Arrhenius relations for diffusivity of oxygen or oxygen-bearing species in silicates or oxides

Phase	Temp. Range (°C)	Medium	$D(cm^2sec^{-1})$ =	Isotopic Method	Data Source
Adularia	350-601	H_2O	4.51×10^{-8} exp(-25.6/RT)	ion-probe	a
Adularia	520-800	KCl	9×10^{-7} exp(-32/RT)	bulk	b
Adularia	400-700	KCl	5.3×10^{-7} exp(-29.6/RT)	bulk	c
Albite	440-805	NaCl	4.5×10^{-5} exp(-37/RT)	bulk	b
Albite	350-800	H_2O	2.31×10^{-9} exp(-21.3/RT)	ion-probe	a
Albite	600-800	NaCl	2.5×10^{-5} exp(-37/RT)	bulk	d
Microcline	400-700	KCl	2.8×10^{-6} exp(-29.6/RT)	bulk	c
Anorthite	350-805	H_2O	1.4×10^{-7} exp(-26.2/RT)	ion-probe	a
Phlogopite	500-800	H_2O, KCl	1×10^{-9} exp(-29/RT)	bulk	e
Magnetite	300-600	H_2O	3.2×10^{-14} exp(-17/RT)	bulk	f
Quartz	1000-1220	O_2	3.7×10^{-9} exp(-55/RT)	bulk	g

(a) Giletti et al. (1978)
(b) Merigoux (1968)
(c) Yund and Anderson (1974)
(d) Anderson and Kasper (1975)
(e) Giletti and Anderson (1975)
(f) Castle and Surman (1969)
(g) Haul and Dumbgen (1962)

Table 4. Summary of K'(a) values estimated for various mineral-water pairs

Mineral Pair (b)	K' 200°	250°	300°	350°	400°
Quartz-Water	1.86	2.01	2.25	2.79	5.06
Albite-Water	1.69	1.82	2.04	2.53	4.59
K-feld-Water	1.55	1.67	1.87	2.32	4.22
Anorthite-Water	1.66	1.80	2.01	2.50	4.54
Muscovite-Water	1.79	1.93	2.16	2.69	4.88
Calcite-Water	1.71	1.85	2.07	2.57	4.65

(a) K' is the equilibrium oxygen isotope partition ratio between solid and water calculated in terms of concentration (see text).

(b) Equilibrium fractionation factors used to calculate the various K' values are derived from Friedman and O'Neil (1977).

Table 5. Summary of times estimated for solid-fluid isotopic exchange in various geologic systems

System (a)	T°C	Phase (b)	r or D (c)	a (d)	W/S (e)	F (f)	~ t(years) (g)
Wairakei, New Zealand	250	Sanidine	9.6×10^{-10}	0.075	2.7-4.5	0.48-0.75	300-700 (2100-2400)
Salton Sea, California	300	Albite	2.6×10^{-8}	0.2	0.8	0.77	40 (125)
Creede, Colorado	250	Sanidine	9.6×10^{-10}	0.01	0.3	0.98	80 (95)
North Pacific sediments	1	Kaolinite	1×10^{-13}	0.00005	75	0.05	660 (66,000)
Glacier Park, Montana	50	Adularia	2.3×10^{-25}	0.0005	0.1	0.934	5.7×10^{8} (4.2×10^{9})
Madoc, Ontario	50	Adularia	2.3×10^{-25}	0.0005	0.1	0.197	1.4×10^{8} (4.2×10^{9})

(a) Isotopic and temperature data on: Wairakei from Clayton and Steiner (1975) and Stewart (1979?), Salton Sea from Clayton et al. (1968), Creede, Colorado from Bethke and Rye (1979), North Pacific sediments from Yeh and Savin (1976), Glacier Park and Madoc from Lawrence and Kastner (1975).

(b) Phases selected that are used to simulate bulk rock-water isotopic rate constants.

(c) Rate constants (r) in moles $m^{-2}sec^{-1}$ used for Wairakei, Salton Sea, Creede and North Pacific sediments, diffusion coefficients (D) used for Glacier Park and Madoc.

(d) Sources of grain radii in cm are: Grindley (1965) for Wairakei, Tewhey (1977) for Salton Sea, Barton et al. (1977) for Creede, Yeh and Savin for North Pacific sediments, and Lawrence and Kastner (1975) for Glacier and Madoc.

(e) Estimation of water/solid oxygen mole ratio discussed in text.

(f) Degree of equilibrium (F) for the hydrothermal systems (Wairakei, Salton Sea, Creede) calculated by procedures discussed in text, F for low temperature systems were calculated by investigators referenced in (a).

(g) Time required in years to attain the values given for F, values in parentheses are times required to achieve equilibrium for the conditions summarized in this table.

Table 6. Summary of run conditions used for hydrogen isotopic exchange experiments described in the literature.

Source (a)	Temperature Range (°C)	Reactants: Solid	Reactants: Solution	Products (b)	Weights: Solid (gm)	Weights: Solution (gm)	Average Particle Size Range (cm) (c)	Average WR/W+R (d)	Average A(m^2) (c)	Time Range (sec)
G/S/H	200-250	Epidote	H_2O	(Epidote)	0.25	0.011	0.0015	3.64×10^{-4}	0.01458	1.38×10^{6} - 6.65×10^{6}
G/S/H	280-550	Zoisite	H_2O	(Zoisite)	0.25	0.011	0.0015	3.99×10^{-4}	0.01558	3.02×10^{5} - 3.28×10^{6}
G/S/H	300	Clinozo	H_2O	(Clinozo)	0.25	0.011	0.0015	3.99×10^{-4}	0.01515	1.99×10^{6}
G/S/H	150	Boehmite	H_2O	(Boehmite)	0.25	0.011	0.0015	9.44×10^{-4}	0.01645	3.2×10^{6}
G/S/H	380	Diaspore	H_2O	(Diaspore)	0.25	0.011	0.0015	9.44×10^{-4}	0.01471	1.21×10^{6}
G/S	250	Epidote	1-4M NaCl	(Epidote)	0.25	0.011	0.0015	3.64×10^{-4}	0.01458	1.3×10^{6} - 2.16×10^{6}
S/E	400-800	Muscovite	H_2O	(Muscovite)	0.2	0.75	0.00565	9.77×10^{-4}	0.00373	1.73×10^{5} - 4.14×10^{6}
S/E	450-750	Biotite	H_2O	(Biotite)	0.2	0.75	0.00565	8.62×10^{-4}	0.00354	7.2×10^{4} - 4.14×10^{6}
S/E	400-670	Hornblende	H_2O	(Hornblende)	0.2	0.75	0.00565	4.66×10^{-4}	0.00331	5.83×10^{5} - 4.14×10^{6}
S/E	570-650	Phlogopite	H_2O	(Phlogopite)	0.2	0.75	0.00565	9.08×10^{-4}	0.00375	3.82×10^{5} - 5.04×10^{5}
S/E	400	Sepentine	H_2O	(Serpentine)	0.2	0.75	0.00565	2.79×10^{-3}	0.00417	5.34×10^{6}
S/E	400	Kaolinite	H_2O	(Kaolinite)	0.2	0.75	0.00565	2.99×10^{-4}	0.00409	5.33×10^{6}
S/E	400	Boehmite	H_2O	(Boehmite)	0.2	0.75	0.00565	3.21×10^{-3}	0.0035	5.33×10^{6}
S/T	97-495	Serpentine	H_2O	(Serpentine)	0.1	0.2	0.0025	1.35×10^{-3}	0.004707	4.39×10^{5} - 1.19×10^{7}
O/K	100-350	Kaolinite	0.04N NaCl	Pyrophyllite + Diaspore	0.15	0.5	$(22 \times 11 \times 13) \times 10^{-4}$	2.2×10^{-4}	0.00536	5.69×10^{6} - 5.05×10^{7}
O/K	100-350	Illite	0.04N NaCl	(Illite)	0.15	0.5	$(22 \times 11 \times 13) \times 10^{-4}$	7.71×10^{-4}	0.00536	5.69×10^{6} - 5.05×10^{7}
O/K	100-350	Mont.	0.04N NaCl	(Mont.)	0.15	0.5	$(22 \times 11 \times 13) \times 10^{-4}$	8.4×10^{-4}	0.00536	5.69×10^{6} - 5.05×10^{7}
K	170-320	Glass-Mont.	H_2O	Mont.	0.05	0.15	0.001 - 0.01 ?	2.8×10^{-4}	$1.15 - 11.5 \times 10^{-3}$	1.73×10^{6} - 6.23×10^{6}
K	170-320	Glass-Kaol.	H_2O	Kaolinite	0.05	0.15	0.001 - 0.01 ?	7.4×10^{-4}	$1.15 - 11.5 \times 10^{-3}$	2.6×10^{6} - 9.24×10^{6}

Table 7. Temperature functions of the hydrogen isotopic rate constants for various mineral-fluid reactions.

Reaction:	Data Source	Log r = (f)	r_g (g)	Activation Energy kJ/mol	Activation Energy kcal/mol
1. Zoisite + H_2O = Zoisite + H_2O	a	-2.72 (1000/T) - 3.635	-0.98	52.1	12.4
2. Epidote + H_2O (NaCl) = Epidote + H_2O (NaCl)	a	-2.475(1000/T) - 3.329	-0.81	47.4	11.3
3. Musc. + H_2O = Musc. + H_2O	b	-3.542(1000/T) - 2.448	-0.98	67.9	16.2
4. Biotite + H_2O = Biotite + H_2O	b	-4.069(1000/T) - 1.208	-0.99	78.0	18.6
5. Phlogopite + H_2O = Phlogopite + H_2O	b	-4.697(1000/T) - 1.012	-1.0	90.0	21.5
6. Hornblende + H_2O = Hornblende + H_2O	b	-4.006(1000/T) - 2.052	-0.94	76.8	18.3
7. Serpentine + H_2O = Hornblende + H_2O	c	-2.103(1000/T) - 2.443	-0.97	40.3	9.6
8. Kaol. + 0.04N NaCl = Pyroph. + Diaspore	d	-1.700(1000/T) - 4.534	-0.97	32.6	7.8
9. Illite + 0.04N NaCl = Illite + 0.04N NaCl	d	-1.088(1000/T) - 6.384	-0.95	20.8	5.0
10. Mont. + 0.04N NaCl = Mont. + 0.04N NaCl	d	-2.101(1000/T) - 3.2103	-0.95	40.3	9.6
11. $Glass_{kaol.}$ + H_2O → Kaol. + H_2O (0.01cm)	e	-1.27 (1000/T) - 3.948	-0.94	24.3	5.8
12. $Glass_{mont.}$ + H_2O → Mont. + H_2O (0.01cm)	e	-3.12 (1000/T) - 0.733	-0.99	60.0	14.3

Notes

Data Source:

(a) Graham et al. (1980)
(b) Suzuoki and Epstein (1976)
(c) Sakai and Tsutsumi (1978)
(d) O'Neil and Kharaka (1976)
(e) Kulla (1979)

(f) Rate constant r is in moles H $m^{-2}sec^{-1}$
(g) r_g is the regression coefficient

Notes

(a) G/S/H = Graham et al. (1980); G/S = Graham and Sheppard (1980); S/E = Suzuoki and Epstein (1976); S/T = Sakai and Tsutsumi (1978); O/K = O'Neil and Kharaka (1976); K = Kulla (1979).

(b) Phases formed either as an alteration product of the reactant or as recrystallized reactant. Phases in parenthesis are for experiments where recrystallization and/or alteration of reactants were not demonstrated.

(c) Particle sizes for epidote, zoisite, clinozoisite, boehmite, diaspore, serpentine, muscovite, phlogopite, hornblende, phlogopite and glass are given as radii assuming a spherical geometry. The lack of photomicrographs or other information detailing the geometry of sheet silicates precluded the use of a more elaborate octagonal plate-geometry calculation for surface area.

(d) The ratio of the product of the number of moles of hydrogen in water (W) and solid (S) to the sum of the number of moles of hydrogen in the system.